

Original Study

Ultrasonographic Assessment and Ocular Biometry of Brown Hawk Owls (*Ninox scutulata*)

Chaeyoung Kwag, Myeongsu Kim, Jae-ik Han, Kichang Lee, and Hakyoung Yoon

Abstract: Ocular trauma is a significant contributor to mortality in wild birds, particularly in owls. Despite the critical role of vision in survival, ocular biometric data for brown hawk-owls (*Ninox scutulata*) remain limited. This study establishes ultrasonographic reference values for ocular structures in the brown hawk-owl. Using B-mode ultrasonography, biometric parameters including corneal thickness, anterior chamber depth, lens thickness, vitreous chamber depth, axial length of the globe, and pecten oculi height were measured in 64 eyes from 32 individuals (26 adults and 6 juveniles). Correlations among these ocular biometric parameters were also analyzed. No significant differences were observed between the left and right eyes or between the horizontal and sagittal imaging planes. However, significant biometric differences were found between adult and juvenile owls, except for pecten oculi height. No significant correlations were identified between body weight and most ocular biometric parameters, except for a slight positive correlation with anterior chamber depth. Axial globe length showed positive correlations with anterior chamber depth, lens thickness, and vitreous chamber depth. Establishing normal ocular biometric values may enhance diagnostic accuracy and will serve as a valuable reference for veterinary ophthalmology, wildlife rehabilitation, and species conservation in brown hawk-owls.

Key words: eye, biometry, ultrasonography, ophthalmic, avian, brown hawk-owl, *Ninox scutulata*

INTRODUCTION

The brown hawk-owl (*Ninox scutulata*) is a migratory, nocturnal raptor that visits the Korean peninsula during the summer breeding season. It is widely distributed across South and Southeast Asia and is designated as a Natural Monument in South Korea.¹ As a mid-level predator, it plays a crucial role in maintaining ecological balance by controlling populations of small mammals and insects.

Ocular trauma is widely recognized as a primary cause of ocular morbidity in wild birds, accounting for nearly 90% of eye disorders diagnosed in raptors. Among these cases, owls represented more than half, highlighting their vulnerability to traumatic ocular

injuries.^{2,3} Given that vision is the most critical sensory modality for owls—essential for nocturnal hunting, navigation, and survival—even minor ocular damage can significantly impair their ability to function in the wild.³ The integrity of the ocular system is an important factor when deciding to release rescued avian species, as it enables them to collect vital information necessary for survival in their natural habitats.^{2,4}

Ocular evaluation methods include physical examination, ophthalmoscopy, and various imaging and other diagnostic modalities, such as electroretinography. Ocular ultrasonography is particularly valuable for assessing intraocular and retrobulbar structures. Numerous studies have been conducted across various animal species to investigate the applications and diagnostic utility of ocular ultrasonography.^{5–20} It is especially indispensable in cases of increased ocular opacity caused by ocular blunt trauma or cataract, as it remains a primary modality for visualizing internal ocular structures, including the anterior chamber, vitreous chamber, and posterior segment.^{5,21}

An accurate assessment of ocular abnormalities using ultrasonography necessitates a comprehensive

From the Department of Veterinary Medical Imaging, College of Veterinary Medicine, Jeonbuk National University, Iksan 54596, Republic of Korea (Kwag, Lee, Yoon); the Laboratory of Wildlife Medicine, College of Veterinary Medicine, Jeonbuk National University, Iksan 54596, Republic of Korea (Kim, Han); and the Jeonbuk Wildlife Center, Jeonbuk National University, Iksan 54596, Republic of Korea (Kim, Han).

Corresponding Author: Hakyoung Yoon, knighttt7240@gmail.com

understanding of the normal anatomical structures of the eye. Therefore, recognizing the normal biometric variations is crucial for accurate interpretation of ultrasonographic findings. Although numerous studies have been conducted on various avian species, including chickens (*Gallus gallus domesticus*), cinereous vultures (*Aegypius monachus*), great grey owls (*Strix nebulosa*), snowy owls (*Bubo scandiacus*), and monk parakeets (*Myiopsitta monachus*), among others,^{21–31} there are no reference values for brown hawk-owls.

This study aimed to report the biometric values for the normal reference range of each ocular parameter and the ultrasonographic features of ocular structures in brown-hawk owls. We hypothesized that ocular biometric parameters would differ between juvenile and adult brown-hawk owls.

MATERIALS AND METHODS

Animals

This study was approved by the Institutional Animal Care and Use Committee of Jeonbuk National University (Iksan-si, Jeollabuk-do, Republic of Korea; Approval No. NON2023-178). Twenty-six adult brown-hawk owls, weighing between 135 and 199 g, and 6 juvenile birds, weighing between 111 and 161 g, from the Jeonbuk Wildlife Center in South Korea (Jeonbuk National University, Iksan-si, South Korea) were examined in this study. These birds were either injured or orphaned and were presented to the center for treatment and rehabilitation. They were housed in aviaries or suitable enclosures and provided with an appropriate carnivorous diet consisting of frozen day-old chicks during their stay. The classification of adults and juveniles was based on feather characteristics. Birds with fully developed, mature plumage were classified as adults, whereas individuals retaining some immature down feathers were categorized as juveniles. All juveniles included in this study were in their hatch year and capable of limited flight. Birds undergoing molt were not considered juveniles because molting typically occurs in post-juvenile or adult stages. The sex of each bird was unknown because this species is not sexually dimorphic. A routine physical examination with ophthalmologic examination, including measuring the pupillary light reflexes and intraocular pressures (IOP; rebound tonometry, Tonovet, iCare, Raleigh, NC, USA), fluorescein staining, and direct ophthalmoscopy (Zumax Veterinary Ophthalmoscope Pro, Zumax Medical, Suzhou, China) was performed. For all IOP measurements, the birds were manually restrained in an upright position with the body gently wrapped in a

towel, taking care to avoid any pressure on the head; neither topical anesthesia nor sedation was used. Examinations were conducted between 9:00 AM and 12:00 PM. Fluorescein staining and pupillary light reflexes testing were normal for all birds included in this study. No significant ocular abnormalities were observed except for minor hemorrhage and debris in a few individuals on direct ophthalmoscopy.

Ultrasonographic examination

A total of 64 eyes underwent B-mode ultrasonographic examination using a 17-MHz hockey stick transducer (Aplio i800; Canon Medical System, Tokyo, Japan). A digital image measurement program (Infinit Vet PACS, Infinit Healthcare Co., Ltd, Seoul, South Korea) was used for all measurements. All birds were gently and manually restrained in an upright (vertical) position. The ultrasonographic examination was performed approximately 30 seconds after instillation of one drop of proparacaine 0.5% (Alcaine eye drops 0.5%; Alcon Korea, Seoul, Korea). No sedation or general anesthesia was used. The transducer was positioned perpendicularly and directly on the cornea with coupling gel (transonic gel; Hansin, Seoul, Korea) for contact in a longitudinal (sagittal plane) and horizontal (dorsal plane) position (Fig 1). Biometric measurements were performed in both longitudinal and horizontal position including corneal thickness (CT), anterior chamber depth (ACD), lens thickness (LT), vitreous chamber depth (VCD), axial length of the globe (ALG), and height of pecten oculi (PH) (Fig 2). Superb microvascular imaging was performed to evaluate blood flow in the pecten oculi using a color velocity scale of 3.1–5.0 cm/s.

Statistical analysis

Descriptive data analysis was performed using computer software (IBM SPSS Statistics 22; IBM Corporation, Armonk, NY, USA). The Kolmogorov-Smirnov test was used to assess normality of the data in both the adult and juvenile groups. The globe and intraocular biometrics were described using the mean, standard deviation (SD), and minimum and maximum values. For comparisons between the horizontal and sagittal planes, as well as between the right eye (OD) and left eye (OS) of the same bird, a paired samples *t*-test was used. An independent samples *t*-test was used to compare measurements between adult and juvenile birds. A value of $P < 0.05$ was considered statistically significant. Additionally, a Pearson bivariate correlation analysis was performed to examine the correlation between weight and each

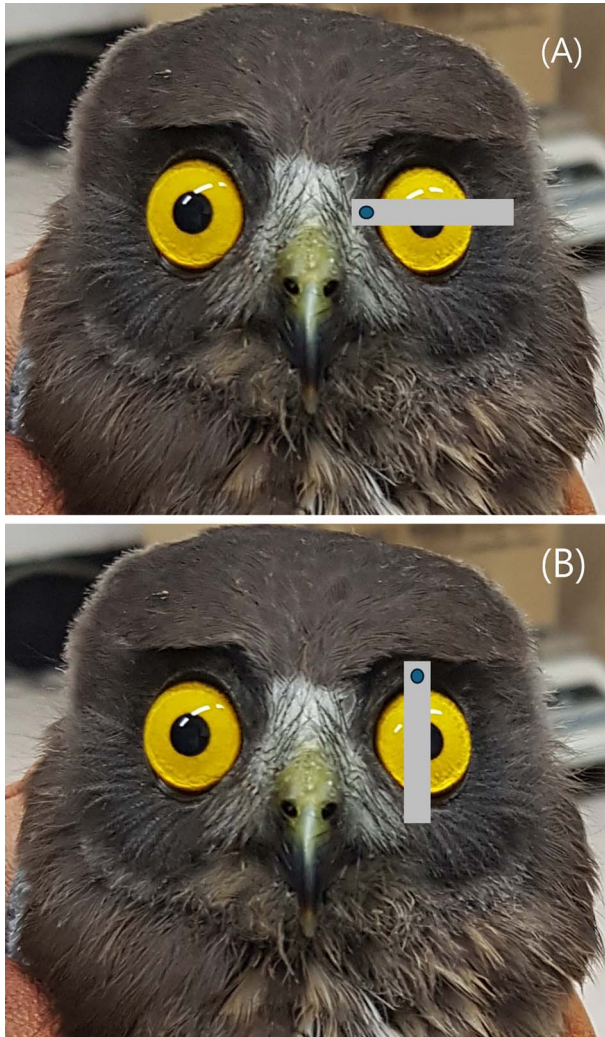


Figure 1. Appearance of brown hawk-owl (*Ninox scutulata*) and the orientation of the ultrasound probe for performing ocular ultrasound. (A) Horizontal plane, and (B) sagittal plane.

biometric measurement, with $P < 0.05$ considered significant.

RESULTS

The ultrasonographic characteristics were remarkably similar among all 64 eyes. The corneal echo was highly reflective and curvilinear, followed by an anechoic region corresponding to the anterior chamber. The lens was visualized as 2 hyperechoic curved lines, representing the anterior and posterior lens capsules, with an anechoic center. The vitreous chamber was anechoic, with the pecten visualized as a moderately echogenic, long, and thin structure. The posterior eye wall, comprising the retina, choroid, and sclera, appeared as a highly reflective, slightly curvilinear

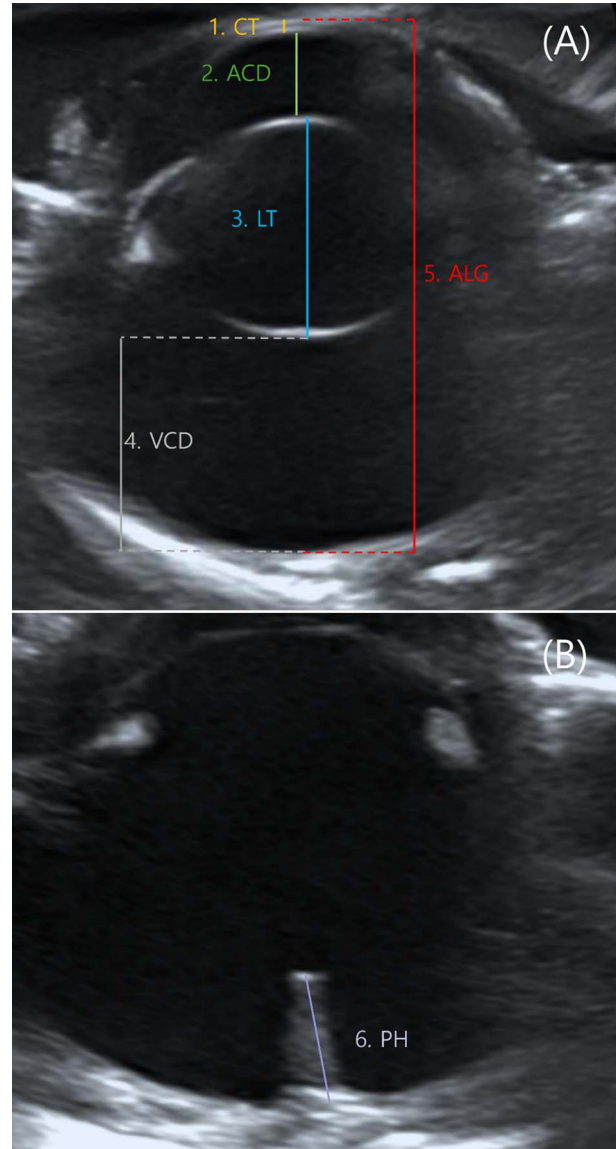


Figure 2. Ultrasonographic appearance of the eye of a normal adult brown hawk-owl (*Ninox scutulata*) and measurements of each biometric parameter. (A) Measurements showing the corneal thickness (CT), anterior chamber depth (ACD), lens thickness (LT), vitreous chamber depth (VCD), and axial length of the globe (ALG), and (B) showing the height of pecten oculi (PH).

echo. It was not possible to separate the retina, choroid, and sclera on ultrasonography. Distal shadowing from the scleral ring hindered visualization of the lateral side of the eyes, preventing accurate measurement and recording of the transverse diameter of the eye and lens (Fig 3).

The IOP results are described in Table 1. Normal reference values for the brown hawk-owls were not previously established; therefore, published IOP values for the Eurasian tawny owl (*Strix aluco*)—reported as

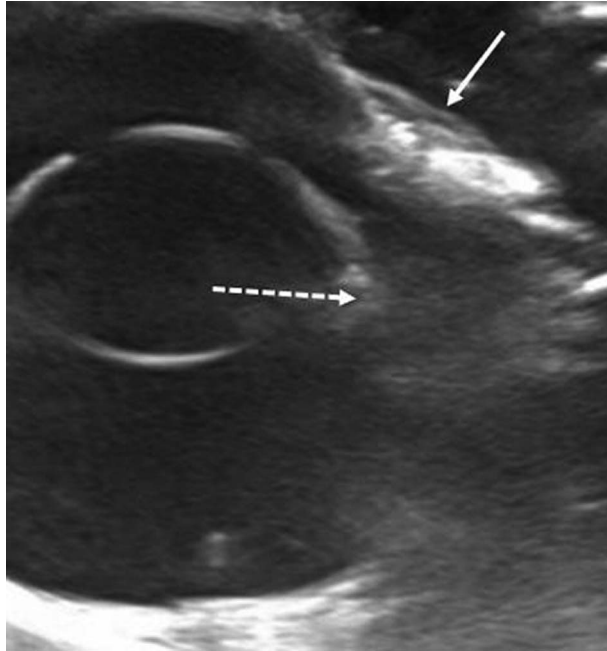


Figure 3. Acoustic shadowing caused by the high reflectivity of the intrascleral ossicle in the eye of a normal adult brown hawk-owl (*Ninox scutulata*). A highly reflective intrascleral ossicle is observed on the lateral side of the eye (solid arrow). Note the acoustic shadowing caused by it (dashed arrow).

9.4 ± 4.1 mm Hg—were used for comparative purposes.^{32,33} The biometric measurements for the sagittal and horizontal planes for both the adults and juveniles are summarized in Table 2.

Based on the paired *t*-test analysis, no statistically significant differences were observed between the left and right eyes for any biometric parameter except for PH, which showed a statistically significant difference between OS and OD in the adult group ($P = 0.014$). All biometric measurements obtained in the sagittal and horizontal planes showed no statistically significant differences (all $P > 0.05$) in either the adults or juveniles.

There was no correlation found between body weight and ocular biometry except for ACD ($r = 0.329$, $P = 0.017$). There were also positive correlations found between ALG and ACD ($r = 0.791$, $P < 0.001$), ALG and LT ($r = 0.540$, $P < 0.001$), and ALG and VCD ($r = 0.499$, $P < 0.001$). When comparing adult birds and juveniles, there were significant differences in all ocular biometrics (all $P < 0.001$), except for PH ($P = 0.368$).

DISCUSSION

This study was performed to establish reference intervals for the size of ocular structures in brown-hawk

Table 1. Intraocular pressure measurements in millimeters of mercury in adult and juvenile brown hawk-owls (*Ninox scutulata*).^a

Age Group	IOP			
	OS		OD	
	Range	Mean \pm SD	Range	Mean \pm SD
Adults (n = 26)	9–13	11.1 \pm 1.47	9–14	11.2 \pm 1.33
Juvenile (n = 6)	7–11	9.0 \pm 1.54	8–11	9.3 \pm 1.50

Abbreviations: IOP, intraocular pressure; OD, right eye; OS, left eye; n, number; SD, standard deviation.

^a Measurements were obtained using rebound tonometry with the birds manually restrained in an upright position.

owls using ocular ultrasonography. Owls are particularly susceptible to ocular injuries due to their distinctive morphological features. Their disc-shaped, frontally oriented faces, combined with a high globe-to-orbit ratio, significantly constrain the space available for extraocular muscles and other orbital soft tissues.² If a collision happens, direct impact on the eye may occur since there is a lack of means for cushioning impact. After a collision event, hyphema and vitreous hemorrhage are common findings in birds,²⁴ which makes intraocular examination impossible with a standard ophthalmoscope.

Ultrasound, which operates by transmitting high-frequency sound waves and analyzing their echoes, is a useful and effective noninvasive method for evaluating ocular structures when anterior segment opacity is present. In avian species, physical adjustment, such as manual restraint, is required for ocular ultrasound evaluation. However, it can be applied without the need for sedation, particularly in brown-hawk owls, as they generally tolerate the stress of handling. A previous study has demonstrated that their heart rate stabilizes significantly over the restraint period.³⁴ Indeed, none of the birds in this study showed any sign of stress, such as anorexia or lethargy, after ocular ultrasonography. However, this may not be true for all owl species undergoing ocular ultrasound.

In B-mode ultrasound, the structures and intraocular chambers of the brown hawk-owl eye were similar to those of other avian and mammalian species. A bony structure called the scleral ring, composed of multiple small ossicles within the sclera and present in birds, reptiles, and many teleost fish—but absent in mammals—creates distal shadowing during ocular ultrasonography (Fig 3). This distal shadowing complicates the measurement of the transverse diameter of the eye and lens, a phenomenon typically observed

Table 2. Ocular biometric measurements of the left and right eyes of brown hawk-owls (*Ninox scutulata*) in the sagittal and horizontal planes.^a

Sagittal Plane								
Adults	OS (n = 26)				OD (n = 26)			
	Mean	SD	Minimum	Maximum	Mean	SD	Minimum	Maximum
CT	0.40	0.02	0.38	0.45	0.41	0.02	0.38	0.46
ACD	2.97	0.21	2.46	3.37	2.98	0.23	2.40	3.31
LT	7.20	0.30	6.47	7.59	7.21	0.28	6.55	7.62
VCD	7.40	0.27	6.91	8.06	7.41	0.26	6.97	8.02
AGL	17.98	0.46	16.39	18.63	17.97	0.47	16.40	18.71
PH	3.15	0.25	2.76	3.69	3.08	0.24	2.52	3.66
Juveniles	OS (n = 6)				OD (n = 6)			
	Mean	SD	Minimum	Maximum	Mean	SD	Minimum	Maximum
CT	0.36	0.01	0.35	0.38	0.36	0.01	0.35	0.37
ACD	2.13	0.40	1.57	2.73	2.03	0.39	1.45	2.57
LT	6.38	0.22	6.09	6.62	6.50	0.22	6.20	6.78
VCD	6.48	0.58	5.80	7.27	6.49	0.48	5.87	7.05
AGL	15.35	1.15	14.14	17.01	15.42	1.05	14.15	16.78
PH	3.06	0.11	2.95	3.20	3.04	0.11	2.86	3.17
Horizontal Plane								
Adults	OS (n = 26)				OD (n = 26)			
	Mean	SD	Minimum	Maximum	Mean	SD	Minimum	Maximum
CT	0.41	0.02	0.37	0.44	0.41	0.02	0.37	0.45
ACD	3.01	0.21	2.47	3.31	3.01	0.21	2.48	3.37
LT	7.21	0.24	6.69	7.68	7.23	0.25	6.68	7.74
VCD	7.37	0.22	6.96	7.95	7.37	0.25	6.87	7.96
AGL	17.98	0.50	16.23	18.67	17.99	0.48	16.31	18.76
PH	3.14	0.25	2.77	3.73	3.08	0.25	2.53	3.70
Juveniles	OS (n = 6)				OD (n = 6)			
	Mean	SD	Minimum	Maximum	Mean	SD	Minimum	Maximum
CT	0.37	0.02	0.35	0.39	0.37	0.03	0.34	0.42
ACD	2.10	0.42	1.45	2.69	2.13	0.44	1.47	2.68
LT	6.39	0.24	6.14	6.78	6.38	0.19	6.16	6.68
VCD	6.41	0.52	5.88	7.00	6.30	0.50	5.86	7.05
AGL	15.31	1.15	14.03	16.89	15.37	1.11	14.12	16.69
PH	3.05	0.11	2.90	3.21	3.04	0.11	2.95	3.19

Abbreviations: OS, left eye; OD, right eye; n, number; CT, corneal thickness; ACD, anterior chamber depth; LT, lens thickness; VCD, vitreous chamber depth; ALG, axial length of the globe; PH, height of pecten oculi; SD, standard deviation.

^a All measurements are in millimeters.

when the eye's diameter is smaller than the transducer size.^{21,23}

We found no significant difference in ocular measurements between data taken from the horizontal and sagittal planes. This suggests that the shape of the eyeball is relatively symmetrical. Therefore, either the horizontal or the sagittal plane can be effectively used for ocular biometry. Variability between the right and left eyes within a single individual is uncommon in the literature,³⁵ and these findings have

been attributed to small sample sizes. Currently, there is no conclusive evidence of significant biometric differences between the right and left eyes in avian species. In this study as well, there was no specific difference between the left and right eyes, which agrees with previous studies in other avian species and mammals.^{6,21,23,36-38} In owls, the asymmetric placement of the external ear openings is a well-known adaptation for sound localization. However, our findings, consistent with other studies, indicate

that this cranial asymmetry does not extend to ocular anatomy: biometric parameters of the left and right eyes show no significant differences, except for measurements in PH. Although a statistically significant difference in PH between the left and right eyes in the adult group was observed, we cannot rule out the possibility that the small sample size may influence this finding, as previous studies have also indicated that results may be affected by limited sample sizes.^{21,39}

We found no significant correlation between body weight and ocular biometric measurements in adult birds, except for a weak but significant positive correlation with ACD. This finding can be interpreted in 2 ways. First, it suggests that ocular structures remain largely consistent among adult birds, reflecting the general uniformity in body size of fully matured brown hawk-owls. Consequently, differences in body weight among adults are unlikely to influence ocular dimensions such as ALG. Second, the relatively small SD of body weights in our sample population indicates that individuals with similar body mass were collected, which may have contributed to the observed lack of correlation with body weight. Given this limitation, future studies with larger sample sizes may be necessary to draw more definitive conclusions.

However, as noted earlier, a slight positive correlation was observed between ACD and body weight. Previous studies in chickens have demonstrated a significant positive correlation between body weight and anterior segment parameters (the cornea-to-anterior lens capsule distance). In contrast, other biometric parameters, including ALG, remained independent of body weight.²² Taken together, these findings suggest that body weight may exert an influence on ACD by modulating aqueous humor dynamics, as previously described in human studies.⁴⁰ These results underscore the potential impact of systemic physiological factors on anterior segment morphology, even in avian species, and highlight the need for further research to elucidate the relationship between body weight and ocular morphometry.

The ALG and the ACD exhibited a positive correlation. Likewise, ALG also demonstrated a positive correlation with LT and VCD. This can be explained by the fact that most of the ocular length is composed of ACD, LT, and VCD, which accounts for the positive correlation between ALG and those parameters. Typically, the eye grows evenly and uniformly as the axial length of the globe increases.⁴¹ This uniform and proportional growth of the eyeball ensures that the structural balance among ocular components is

maintained as the eye develops. Because ACD, LT, and VCD constitute most of the axial length, their enlargement is a natural consequence of overall ocular growth. This proportionality is crucial for preserving the optical and functional properties of the eye, such as maintaining proper refractive focus.⁴² Without such synchronized growth, imbalances in ocular dimensions could lead to refractive errors or compromise the stability of the eye's architecture. The expansion of ACD, LT, and VCD as integral parts of axial length reflects the eye's need to adapt uniformly during development to ensure both visual efficiency and mechanical integrity.

The pecten oculi is a vascularized structure in the avian eye that supplies oxygen and nutrients to the retina. Because birds lack retinal blood vessels,⁴³ it plays a crucial role in maintaining visual function. Its unique structure and function are important in ophthalmology. Evaluation of the size and shape of the pecten oculi using ultrasound is reported in multiple raptor species.^{24,38,44–50} Although recent advances in imaging technology suggest the potential to visualize the pecten oculi with ocular computed tomography and magnetic resonance imaging, previous studies have consistently reported that it cannot be seen with these modalities. Given the increasing capabilities of high-resolution imaging equipment, further studies using such advanced technologies are necessary to explore the visualization and structural analysis of the pecten oculi. Ocular ultrasound remains the only reliable modality for diagnosing pecten lesions, particularly when opacities are present in the anterior segment of the eye.^{21,27,38,51} Accurate observation and clinical diagnosis require a thorough understanding of the morphologic features and biometric data of the pecten, just as with many other ocular parameters.⁴⁵

When the pecten oculi is partially or completely ruptured, it may lose its normal morphology and blood flow pattern, and its length may also be reduced.⁴⁴ Assessing the normal size, appearance, and Doppler flow pattern of the pecten oculi is essential for evaluating its structural integrity, particularly in cases of head trauma or vitreous hemorrhage. The ultrasonographical feature of the pecten in brown hawk-owls was moderately echogenic with smooth margins. The pecten exhibited a thin, tall morphology, contrasting with the previously documented broad, plane shape observed in some other nocturnal birds.^{38,39} A flame-like blood flow pattern was identifiable along the longitudinal axis of the pecten on superb microvascular imaging.

When comparing adults and juveniles, significant differences in ocular biometric parameters, except PH, were observed, suggesting distinct growth-related biometric characteristics. In juvenile birds, all measured parameters, except for PH, exhibited shorter distances between anatomical structures compared to adults. This finding indicates that most ocular structures continue to grow as the bird matures, while the development of the pecten oculi may be completed early during the juvenile stage.⁵² Initially, we planned to reassess the biometric data, especially for the pecten oculi, after the juveniles had fully matured. However, owing to a decision made by the wildlife rescue center, they were released into the wild before reaching adulthood to facilitate early adaptation to their natural environment.^{31,53–55} Despite this limitation, the observed stability in PH values across age groups strongly supports the hypothesis that the growth of the pecten oculi is finalized during the juvenile stage, and this finding is consistent with previous studies conducted in other species.⁵²

There were several limitations in this study. First, brown hawk-owls are migratory birds that visit Korea only during the summer, and their migratory route includes regions such as Southeast Asia, India, and Sri Lanka,^{56,57} making it challenging to obtain an adequate sample size. Future studies could benefit from obtaining a larger sample size across the species' migratory range to improve the robustness of the findings. Second, because the species does not exhibit sexual dimorphism, it was not possible to investigate differences between males and females. Other techniques, such as endoscopic examination or behavior-based sexing, were also not considered due to their limited applicability to the study's noninvasive imaging approach. In particular, behavior-based sexing was not feasible, as the subjects were rescued wild individuals undergoing rehabilitation, making consistent behavioral assessment difficult. Some studies have used polymerase chain reaction assays to determine the sex of individual birds.²¹ However, in this study, polymerase chain reaction assays were not performed due to limitations in resources, such as the availability of genetic testing facilities and budgetary constraints. Additionally, the focus of this research was on broader biometric parameters rather than sex-specific differences, making polymerase chain reaction testing less critical for the primary objectives. Third, only healthy birds were included in this study, as the purpose was to establish a normal reference range. Consequently, it was not possible to compare the findings with changes observed in birds with ocular abnormalities. Future studies comparing ocular

abnormalities could provide valuable insights, potentially aiding in the diagnosis of these conditions. Finally, as previously mentioned, follow-up observations were not feasible after their release into the wild, thereby preventing the assessment of growth-associated changes.

This study is the first to establish normal reference intervals for ocular biometrics in brown hawk-owls using B-mode ultrasonography. Given the significant variability in biometric values across bird species, species-specific studies are essential to develop accurate reference intervals for diagnosing ocular lesions. Additionally, further research with larger sample sizes is necessary to validate and expand upon the findings of this study.

Acknowledgments: This study was supported by the National Institute of Wildlife Disease Control and Prevention as "Specialized Graduate School Support Project for Wildlife Disease Specialists."

REFERENCES

1. Lee S, Shin Y. A current status of natural heritage using the bird's carcasses in South Korea. *J Korean Instit Trad Landscape Architect*. 2021;39:50–54.
2. Moore BA, Teixeira LBC, Sponsel WE, et al. The consequences of avian ocular trauma: histopathological evidence and implications of acute and chronic disease. *Vet Ophthalmol*. 2017;20:496–504.
3. Holt DW, Layne EA. Eye injuries in long-eared owls (*Asio otus*): prevalence and survival. *J Raptor Res*. 2008;42:243–247.
4. Martin GR. What drives bird vision? Bill control and predator detection overshadow flight. *Front Neurol Neurosci Res*. 2017;11:619.
5. Kim Y, Kim B, Lee K, et al. Ultrasonographic assessment of ocular parameters in dogs: effects of weight and breed, controlled for BCS and age. *Front Vet Sci*. 2024;11.
6. Schiffer SP, Rantanen NW, Leary GA, et al. Biometric study of the canine eye, using A-mode ultrasonography. *Am J Vet Res*. 1982;43:826–830.
7. Silva EG, Pessoa GT, Moura LS, et al. Biometric, B-mode and color Doppler ultrasound assessment of eyes in healthy dogs. *Pesqui Vet Bras*. 2018;38:565–571.
8. Ngamrojanavanit N, Tanthasathien N, Srisamai N, et al. The use of B-scan coupling with A-scan ultrasonography to characterize ocular biometry in canine absolute glaucoma. *Wetchasan Sattawaphaet*. 2019;49:273–281.
9. Boroffka SA, Voorhout G, Verbruggen A-M, et al. Intraobserver and interobserver repeatability of ocular biometric measurements obtained by means of B-mode ultrasonography in dogs. *Am J Vet Res*. 2006;67:1743–1749.
10. Santos M, Zacarias A, Porto E, et al. Ocular echobiometry and relationship with cranial and body morphometric parameters in Shih Tzu dogs. *Arq Bras Med Vet Zootec*. 2022;74:807–813.

11. Audu H, Idris S, Hamidu A, et al. Sonographic measurements of ocular biometry of indigenous Nigerian dogs in Zaria, Nigeria. *Niger Vet J.* 2017;38:140–150.
12. Andrade TF, Moreno L, Nascimento FF, et al. Ocular biometry and ophthalmic parameters of normal eyes in French bulldog healthy dogs. *Adv Anim Vet Sci.* 2020;9:438–441.
13. McMullen RJ, Gilger BC. Keratometry, biometry and prediction of intraocular lens power in the equine eye. *Vet Ophthalmol.* 2006;9:357–360.
14. Herbig L. Ultrasonographic biometry of the growing equine eye and examination of the diseased cornea with high-frequency ultrasound and ultrasound biomicroscopy. Freien Universität Berlin. 2017. Thesis.
15. Mirshahi A, Shafigh S, Azizzadeh M. Ultrasonographic biometry of the normal eye of the Persian cat. *Aust Vet J.* 2014;92:246–249.
16. Owens CD, Michau TM, Boorstein J, et al. Keratometry, biometry, and prediction of intraocular lens power in adult tigers (*Panthera tigris*). *Am J Vet Res.* 2022;83:140–146.
17. Agostinho ICC, Martins JA, Balbuena MCS, et al. Ocular biometry of snakes of the species *Python bivittatus* kept in captivity. *Braz J Vet Res Anim Sci.* 2023;60:e213344–e213344.
18. Oriá AP, Oliveira AVD, Pinna MH, et al. Ophthalmic diagnostic tests, orbital anatomy, and adnexal histology of the broad-snouted caiman (*Caiman latirostris*). *Vet Ophthalmol.* 2015;18:30–39.
19. Khorrami-Nejad M, Khodair AM, Khodaparast M, et al. Comparison of the ocular ultrasonic and optical biometry devices in the different quality measurements. *J Optom.* 2023;16:284–295.
20. Ruiz T, Campos WN, Peres TP, et al. Intraocular pressure, ultrasonographic and echobiometric findings of juvenile Yacare caiman (*Caiman yacare*) eye. *Vet Ophthalmol.* 2015;18:40–45.
21. Apruzzese A, Rodriguez A, Gonzalez F, et al. Ocular ultrasonography and biometry in the cinereous vulture (*Aegypius monachus*). *J Avian Med Surg.* 2018;32:307–313.
22. Nardi S, Puccini Leoni F, Monticelli V, et al. Tear production, intraocular pressure, ultrasound biometric features and conjunctival flora identification in clinically normal eyes of two Italian breeds of chicken (*Gallus gallus domesticus*). *Animals (Basel).* 2021;11:2987.
23. Squarzoni R, Perlmann E, Antunes A, et al. Ultrasonographic aspects and biometry of striped owl's eyes (*Rhinoptynx clamator*). *Vet Ophthalmol.* 2010;13:86–90.
24. Wills S, Pinard C, Nykamp S, et al. Ophthalmic reference values and lesions in two captive populations of northern owls: great grey owls (*Strix nebulosa*) and snowy owls (*Bubo scandiacus*). *J Zoo Wildl Med.* 2016;47:244–55.
25. Halsmer EL, Heatley JJ, Scott EM. Clinical ophthalmic parameters of the quaker parrot (*Myiopsitta monachus*). *Vet Ophthalmol.* 2023;26:428–439.
26. Simonis KM, Baron HR, Wernery U, et al. Characterization of ophthalmic lesions and normal ocular parameters in a flock of captive MacQueen's (*houbara*) bustards (*Chlamydotis macqueenii*). *Vet Ophthalmol.* 2025;28:574–582.
27. Sharma A, Sood S, Pandey P, et al. Ocular ultrasonography and biometry of healthy eyes in white leghorn birds. *J Anim Res* 2021;11:733–736.
28. Hwang J, Kang S, Seok S, et al. Imaging characteristics of the eyes of cinereous vulture (*Aegypius monachus*): morphology and comparative biometric measurement. *J Vet Med Sci.* 2021;83:1330–1337.
29. Presby JA, Scott EM, Norman KN, et al. Normative ocular data for juvenile and adult Japanese quail (*Coturnix japonica*). *Vet Ophthalmol.* 2020;23:526–533.
30. Lehmkuhl RC, Almeida MF, Mamprim MJ, et al. B-mode ultrasonography biometry of the Amazon parrot (*Amazona aestiva*) eye. *Vet Ophthalmol.* 2010;13:26–28.
31. Meekins JM, Stuckey JA, Carpenter JW, et al. Ophthalmic diagnostic tests and ocular findings in a flock of captive American flamingos (*Phoenicopterus ruber ruber*). *J Avian Med Surg.* 2015;29:95–105.
32. Reuter A, Müller K, Arndt G, et al. Reference intervals for intraocular pressure measured by rebound tonometry in ten raptor species and factors affecting the intraocular pressure. *J Avian Med Surg.* 2011;25:165–172.
33. Carter RT, Lewin AC. Ophthalmic evaluation of raptors suffering from ocular trauma. *J Avian Med Surg.* 2021;35:2–27.
34. Doss GA, Mans C. The effect of manual restraint on physiological parameters in barred owls (*Strix varia*). *J Avian Med Surg.* 2017;31:1–5.
35. Kuhn SE, Hendrix DV, Jones MP, et al. Biometry, keratometry, and calculation of intraocular lens power for the bald eagle (*Haliaeetus leucocephalus*). *Vet Ophthalmol.* 2015;18:106–112.
36. Montiani-Ferreira F, Truppel J, Tramontin MH, et al. The capybara eye: clinical tests, anatomic and biometric features. *Vet Ophthalmol.* 2008;11:386–394.
37. Zhou X, Qu J, Xie R, et al. Normal development of refractive state and ocular dimensions in guinea pigs. *Vision Res.* 2006;46:2815–2823.
38. Gumpenberger M, Kolm G. Ultrasonographic and computed tomographic examinations of the avian eye: physiologic appearance, pathologic findings, and comparative biometric measurement. *Vet Radiol Ultrasound.* 2006;47:492–502.
39. Beckwith-Cohen B, Horowitz I, Bdoлах-Abram T, et al. Differences in ocular parameters between diurnal and nocturnal raptors. *Vet Ophthalmol.* 2015;18:98–105.
40. Toptan M, Elkan H, Erdogdu H, et al. The effects of metabolic and bariatric surgery on the anterior segment parameters of the eye. *Obesity Surg.* 2025:1–8.
41. Huang Z, Qi J, Cheng K, et al. The relationships between lens diameter and ocular biometric parameters: an ultrasound biomicroscopy-based study. *Front Med (Lausanne).* 2023;10:1306276.
42. Zhang Z, Mu J, Wei J, et al. Correction: Correlation between refractive errors and ocular biometric parameters in children and adolescents: a systematic review and meta-analysis. *BMC Ophthalmol.* 2023;23:496.

43. Ruggeri M, Major JC, McKeown C, et al. Retinal structure of birds of prey revealed by ultra-high resolution spectral-domain optical coherence tomography. *Invest Ophthalmology Visual Sci.* 2010;51:5789–5795.
44. Labelle AL, Whittington JK, Breaux CB, et al. Clinical utility of a complete diagnostic protocol for the ocular evaluation of free-living raptors. *Vet Ophthalmol.* 2012; 15:5–17.
45. Ferreira TAC, Fornazari G, Saldanha A, et al. The use of sulfur hexafluoride microbubbles for contrast-enhanced ocular ultrasonography of the pecten oculi in birds. *Vet Ophthalmol.* 2019;22:423–429.
46. Kiliç B, Toprak B, Yüksel S, et al. Morphological features of the pecten oculi in the common kestrel (*Falco tinnunculus*). *Anat Histol Embryol.* 2025;54: e70015.
47. Ince NG, Onuk B, Kabak YB, et al. Macroanatomic, light, and electron microscopic examination of pecten oculi in the seagull (*Larus canus*). *Microscopy Res Tech.* 2017;80:787–792.
48. Orhan İÖ, Ekim O, Bayraktaroglu AG. Morphological investigation of the pecten oculi in quail (*Coturnix coturnix japonica*). *Vet Fak Derg.* 2011;58:5–10.
49. Gültiken ME, Yıldız D, Onuk B, et al. The morphology of the pecten oculi in the common buzzard (*Buteo buteo*). *Vet Ophthalmol.* 2012;15:72–76.
50. Rajab JM. Morphological and histological description of the pecten oculi in the sparrow hawk (*Accipiter nisus*). *Diyala J Pure Sci.* 2012;8:27–29.
51. Morgan RV, Donnell RL, Daniel GB. Magnetic resonance imaging of the normal eye and orbit of a screech owl (*Otus asio*). *Vet Radiol Ultrasound.* 1994;35:362–367.
52. El-Din EYS, Dakrory AI. Early anatomical and embryological description of pecten oculi in cattle egret (*Bubulcus ibis*). *J Adv Zool.* 2016;37:14–20.
53. Klingbeil N, Nuzzo J, Seitz D, et al. Length of stay in rehabilitation influences magnitude of the acute stress response in birds of prey. *Wildl Rehab Bull.* 2024;42: 50–59.
54. Bussolini LT, Franks VR, Heinsohn R, Effects of age and captivity on the social structure and migration survival of a critically endangered bird. *Animal Conserv.* 2024;27:671–684.
55. Pritchard RA, Kelly EL, Biggs JR, et al. Identifying cost-effective recovery actions for a critically endangered species. *Conserv Sci Pract.* 2022;4:e546.
56. Kim HK. Food-niche partition and sexual dimorphism of Northern boobooks (*Ninox japonica*) and Oriental scops owls (*Otus sunia*) in Korea. Seoul National University; 2015. Thesis.
57. Byun HR, Rieu MS, Han SW, et al. Ixodid ticks from wild and domestic animals in East and Central Asian flyways. *Acta Trop.* 2024;249:107091.